KU LEUVEN

Citation	Dora Turk, Joris Gillis, Goele Pipeleers, Jan Swevers (2016), **Experimental validation of a regularized nonlinear least-squares-based identification approach for linear parameter-varying systems** Proceedings of ISMA 2016 - International Conference on Noise and Vibration Engineering, Leuven, Belgium, September 19-21, 2016.
Archived version	Author manuscript: the content is identical to the content of the published paper, but without the final typesetting by the publisher
Published version	https://www.isma-isaac.be/proceedings/papers/isma2016_0551.pdf
Journal homepage	https://www.isma-isaac.be/proceedings/Webstart.html
Author contact	dora.turk@kuleuven.be *+ 32 (0)16 372857*
IR	https://lirias.kuleuven.be/handle/123456789/548379

(article begins on next page)

Experimental validation of a regularized nonlinear least-squares-based identification approach for linear parameter-varying systems

D. Turk [1], **J. Gillis** [1], **G. Pipeleers** [1], **J. Swevers** [1]
[1] KU Leuven, Department of Mechanical Engineering, *Member of Flanders Make*
Celestijnenlaan 300 B, B-3001, Heverlee, Belgium
e-mail: **dora.turk@kuleuven.be**

Abstract
This paper presents a regularized nonlinear least-squares-based identification method for linear parameter-varying (LPV) systems. The objective of the method is, on one hand, to obtain an LPV model the response of which as accurately as possible fits the measured response generated by the system to be identified. On the other hand, by introducing $\ell_{2,1}$-norm regularization of the model matrices the method prefers models with a dependency on the scheduling parameter that is as simple as possible. The optimal model is therefore one that satisfies both criteria. The experimental validation on a mechatronic XY-motion system shows that through $\ell_{2,1}$-norm regularization, a sparse model is obtained with a smoother evolution of its poles and zeros, compared to the model obtained without regularization. This is at the cost of only very limited loss of model accuracy.

1 Introduction

Linear parameter-varying (LPV) systems are nonlinear systems described by a linear model with coefficients varying as a function of one or more scheduling parameters. These time-varying parameters determine the system's operating point. The inherited features of the well-studied linear time-invariant (LTI) systems make LPV systems attractive for modern industrial control, with main applications in aircrafts, robotics, and wind turbines.

The literature on LPV system identification distinguishes between a global and local approach. The global techniques (e.g. [1,2]) directly identify an LPV model based on data obtained from an experiment where both the input signal and scheduling parameters are continuously changing. Experiments of this kind are referred to as global experiments. The local identification techniques (e.g. [3,4]) typically consist of two steps. In the first step, several LTI models are identified based on local input-output data obtained for various fixed values of the scheduling parameters (local experiments). These LTI models are in the second step interpolated, yielding a parameter dependent model.

Both approaches have their advantages and disadvantages. The global approach aims at optimizing model accuracy under changing scheduling parameter conditions. In addition, dynamic scheduling dependency - dependency on time-shifted instances of the scheduling parameters - can only be detected through a global identification experiment. The local approach can only identify systems with static scheduling dependency - in which the system depends solely on the instantaneous time values of the scheduling parameters, but can to a large extent rely on the well-studied LTI identification methods.

Although different, data originating from global and local experiments both provide valuable information that, when combined, gives a more complete picture of the system at hand. This hypothesis led to the combined global and local approach [5]. As a sequel, this paper validates the approach experimentally on

a mechatronic XY-motion system and, in addition, proposes an $\ell_{2,1}$-norm regularization to avoid ending up with an excess of degrees of freedom, possibly leading to overfitting.

The paper is organized as follows. Section 2 describes the chosen LPV model structure. Section 3 introduces the combined global and local identification method, firstly the nonregularized version and secondly the version with the $\ell_{2,1}$-norm regularization. Section 4 discusses the experimental validation and comparison of both the regularized and nonregularized nonlinear least-squares LPV identification method. The obtained results form the bottom line for the conclusions conveyed in Section 5.

2 LPV model structure

In this paper we use the following fully parameterized discrete time LPV model:

$$\begin{cases} x(t+1) = (\mathscr{A} \diamond p)(t) \cdot x(t) + (\mathscr{B} \diamond p)(t) \cdot u(t) \\ y(t) = (\mathscr{C} \diamond p)(t) \cdot x(t) + (\mathscr{D} \diamond p)(t) \cdot u(t), \end{cases} \tag{1}$$

where $x(t) \in \mathbb{R}^n$, $u(t) \in \mathbb{R}^r$, $y(t) \in \mathbb{R}^l$, and $p(t) \in \mathbb{R}^{N_p}$, are respectively the state vector, the input vector, the output vector, and the scheduling parameter vector, at time instance t.

The state-space matrices of the introduced model are parameter-dependent:

$$(\mathscr{A} \diamond p)(t) = A_0 + \sum_{i=1}^{N_b} A_i f_i(p(t), ..., p(t-n_d)),$$

$$(\mathscr{B} \diamond p)(t) = B_0 + \sum_{i=1}^{N_b} B_i f_i(p(t), ..., p(t-n_d)),$$

$$(\mathscr{C} \diamond p)(t) = C_0 + \sum_{i=1}^{N_b} C_i f_i(p(t), ..., p(t-n_d)),$$

$$(\mathscr{D} \diamond p)(t) = D_0 + \sum_{i=1}^{N_b} D_i f_i(p(t), ..., p(t-n_d)),$$

where $A_0 \in \mathbb{R}^{n \times n}$, $A_i \in \mathbb{R}^{n \times n}$, $B_0 \in \mathbb{R}^{n \times r}$, $B_i \in \mathbb{R}^{n \times r}$, $C_0 \in \mathbb{R}^{l \times n}$, $C_i \in \mathbb{R}^{l \times n}$, $D_0 \in \mathbb{R}^{l \times r}$, $D_i \in \mathbb{R}^{l \times r}$; N_b is the number of basis functions f_i employed for parameterization, and n_d is the number of time-shifts of the scheduling parameters. It is here for brevity taken that N_b and n_d are equal for all model matrices $\{A, B, C, D\}$. This, however, does not necessarily always hold.

3 Combined global and local identification approach

3.1 Nonlinear least-squares problem

Local identification data can be either time or frequency domain data. Global identification data are in most cases time domain data, although there are global identification methods that consider frequency domain data, e.g. [6], provided that the input and scheduling are chosen to be periodic and synchronized. In this paper, we only use global identification data in time domain.

Assume that N_t different sets of time domain data and N_f different sets of frequency domain data are available. First consider time domain data, which can originate from either local or global experiments. The difference between the response $\mathbf{y}^{q_\mathrm{t}}(\Theta)$ of the LPV model (1) to the input of the q_t^{th} experiment, and the measured output $\mathbf{y}_\mathrm{m}^{q_\mathrm{t}}$, equals:

$$\boldsymbol{\varepsilon}_{\mathrm{t}}^{q_{\mathrm{t}}}(\Theta) = \mathbf{y}^{q_{\mathrm{t}}}(\Theta) - \mathbf{y}_{\mathrm{m}}^{q_{\mathrm{t}}}, \tag{2}$$

where

$$\Theta = [vec(A);\ vec(B);\ vec(C);\ vec(D)]. \tag{3}$$

Second assume N_{f} local experiments providing frequency domain data. The difference between the system's complex frequency response function (FRF) $\mathbf{G}_{\mathrm{m}}^{\mathbf{q}_{\mathrm{f}}}$ resulting from the q_{f}^{th} local experiment and the corresponding model FRF $\mathbf{G}^{q_{\mathrm{f}}}(\Theta)$ equals:

$$\boldsymbol{\varepsilon}_{\mathrm{f}}^{q_{\mathrm{f}}}(\Theta) = \mathbf{G}^{q_{\mathrm{f}}}(\Theta) - \mathbf{G}_{\mathrm{m}}^{q_{\mathrm{f}}}. \tag{4}$$

A nonlinear least-squares criterion that combines global and local experiments, from the time and frequency domain, can now be formulated:

$$V_{\mathrm{NLS}}(\Theta) = \frac{1}{2}\left(\sum_{q_{\mathrm{t}}}(\boldsymbol{\varepsilon}_{\mathrm{t}}^{q_{\mathrm{t}}}(\Theta))^{\mathrm{T}} W_{\mathrm{t}}^{q_{\mathrm{t}}} \boldsymbol{\varepsilon}_{\mathrm{t}}^{q_{\mathrm{t}}}(\Theta) + \sum_{q_{\mathrm{f}}}(\boldsymbol{\varepsilon}_{\mathrm{f}}^{q_{\mathrm{f}}}(\Theta))^{\mathrm{H}} W_{\mathrm{f}}^{q_{\mathrm{f}}} \boldsymbol{\varepsilon}_{\mathrm{f}}^{q_{\mathrm{f}}}(\Theta)\right). \tag{5}$$

The weighting matrices W_{t} and W_{f} serve to emphasize a time span or a frequency range of interest, respectively. In case no specific weighting is required, a constant that normalizes the time/frequency domain error is recommended, that is:

$$W_{\mathrm{t}}^{q_{\mathrm{t}}} = \left(\sum_{q_{\mathrm{t}}} \|\mathbf{y}_{\mathrm{m}}^{q_{\mathrm{t}}}\|^2\right)^{-1}, \tag{6}$$

$$W_{\mathrm{f}}^{q_{\mathrm{f}}} = \left(\sum_{q_{\mathrm{f}}} \|\mathbf{G}_{\mathrm{m}}^{q_{\mathrm{f}}}\|^2\right)^{-1}. \tag{7}$$

The optimal set of parameter estimates Θ^* is then the one that minimizes (5), i.e.

$$\Theta^* = arg\min_{\Theta} V_{\mathrm{NLS}}. \tag{8}$$

The solution of such a problem is typically obtained using the Levenberg-Marquardt algorithm and this paper is no exception.

3.2 Second-Order Cone Programming (SOCP) problem

Selecting an adequate set of basis functions is very challenging and time-consuming, particularly if no information on the scheduling parameter dependency of the system model is available. This issue has been widely discussed (see e.g. [7, 8]). The approach chosen to tackle it in this paper is to propose a large set of basis functions based on physical insights and a trial-and-error procedure, and extract an adequate subset by applying $\ell_{2,1}$-norm regularization to the estimation problem. The $\ell_{2,1}$-norm of an arbitrary matrix $M \in \mathbb{R}^{m\times n}$ is defined as

$$\|M\|_{2,1} = \sum_{j=1}^{n}\sqrt{\sum_{i=1}^{m} M(i,j)^2}, \tag{9}$$

and has a desirable "grouping" property: in case (9) would be added to an optimization problem where all elements of M are optimization variables, the optimization favors solutions M with as many zero columns as possible. In this paper we extend the concept of columns in (9) to the matrix blocks associated with the same basis functions, in order to obtain an algorithm that eventually discards redundant parameters. The regularization term added to the NLS criterion (5) is therefore

$$V_{\text{reg}}(\Theta) = \gamma \sum_{i=1}^{N_b} \left(\|vec(A_i)\|_2 + \|vec(B_i)\|_2 + \|vec(C_i)\|_2 + \|vec(D_i)\|_2 \right), \tag{10}$$

where γ is a scalar, the value of which determines the importance of the regularization with regard to the model accuracy, and *vec* stands for matrix vectorization. The optimal set of parameters is now one that minimizes the updated criterion:

$$\Theta^* = arg \min_{\Theta} (V_{\text{NLS}}(\Theta) + V_{\text{reg}}(\Theta)). \tag{11}$$

Due to a nonquadratic nature of (10), the optimization problem (11) cannot be solved by the Levenberg-Marquardt algorithm. However, having it reformulated into

$$\begin{aligned} \underset{\Theta,\, s}{\text{minimize}} \quad & V_{\text{NLS}}(\Theta) + \gamma \sum_{i=1}^{N_b} \left(s_i^A + s_i^B + s_i^C + s_i^D \right) \\ \text{subject to} \quad & \|vec(A_i)\|_2 \leq s_i^A \\ & \|vec(B_i)\|_2 \leq s_i^B \\ & \|vec(C_i)\|_2 \leq s_i^C \\ & \|vec(D_i)\|_2 \leq s_i^D \\ & i = 1, ..., N_b \end{aligned} \tag{12}$$

one can recognize a nonlinear second-order cone programming (NSOCP) problem, [9]. In [10], a sequential quadratic programming (SQP)-type algorithm for solving such problems is proposed. This algorithm solves a convex SOCP subproblem in each iteration, with the constraints being linear approximations of the constraint functions of the original problem, and with a convex quadratic function as the objective function. The same principle is adopted here, but remaining withing the Levenberg-Marquardt framework. Namely, in each iteration k the step $\Delta\Theta$ is calculated by solving the following subproblem:

$$\begin{aligned} \underset{\Delta\Theta,\, \Delta s}{\text{minimize}} \quad & \nabla V_{\text{NLS}}(\Theta^k)^T \Delta\Theta + \frac{1}{2} \Delta\Theta^T M_k \Delta\Theta + \gamma \sum_{i=1}^{N_b} \left(\Delta s_i^A + \Delta s_i^B + \Delta s_i^C + \Delta s_i^D \right) \\ \text{subject to} \quad & \|vec(A_i^k + \Delta A_i^k)\|_2 \leq s_i^{A,k} + \Delta s_i^A \\ & \|vec(B_i^k + \Delta B_i^k)\|_2 \leq s_i^{B,k} + \Delta s_i^B \\ & \|vec(C_i^k + \Delta C_i^k)\|_2 \leq s_i^{C,k} + \Delta s_i^C \\ & \|vec(D_i^k + \Delta D_i^k)\|_2 \leq s_i^{D,k} + \Delta s_i^D \\ & i = 1, ..., N_b \end{aligned} \tag{13}$$

using the Embedded Conic Solver (ECOS) [11]. In (13), M_k is a Hessian approximation matrix defined as in the original Levenberg-Marquardt version:

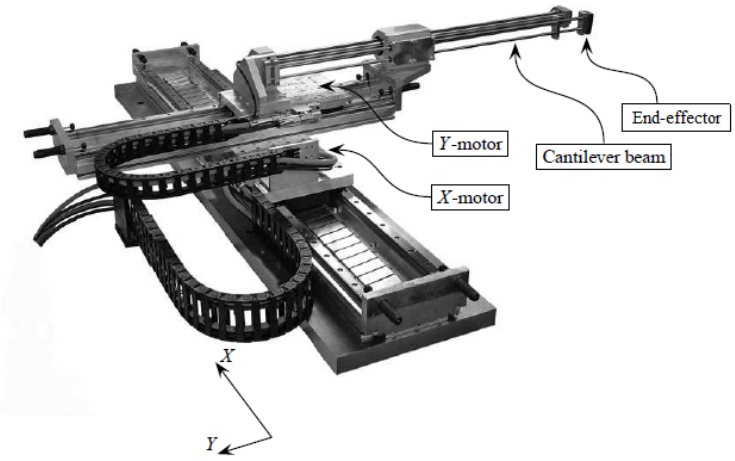

Figure 1: XY-motion system

$$M_k = \nabla V_{\mathrm{NLS}}(\Theta^k)^T \nabla V_{\mathrm{NLS}}(\Theta^k) + \lambda^2 \mathrm{diag}(\nabla V_{\mathrm{NLS}}(\Theta^k)^T \nabla V_{\mathrm{NLS}}(\Theta^k)), \tag{14}$$

where $\nabla V_{\mathrm{NLS}}(\Theta^k)$ is the Jacobian matrix, and λ is the damping parameter. The algorithm is stopped once the step size is smaller than a specified threshold or after a sufficient improvement in the model performance/sparsity has been reached.

4 Experimental validation: Identification of an XY-motion system

4.1 Setup description

The system under test is the XY-motion system shown in Fig. 1. The system consists of two perpendicularly mounted linear stages and a flexible cantilever beam. The length of this beam is changed by the position of the Y-motor, such that the cantilever beam resonances and hence the dynamics of the XY-motion system in the X-direction depend on the position of the Y-motor [12]. The reference position for the position controller of the Y-motor can thus be seen as a scheduling parameter of the system we aim to identify. The reference velocity for the velocity controller of the X-motor is the system input, while the acceleration of the end-effector in the same direction represents the system output. The acceleration is measured by a MEMS accelerometer designed to measure low frequency vibration and motion, and having a flat frequency spectrum within $f \in [0, 250]$ Hz. The estimated signal-to-noise (SNR) ratio is 47 dB.

4.2 Experiment design

The assessment of the proposed approach involves global and local experiments. All experiments were executed at sampling rate $f_s = 1$ kHz. In the global experiment, the system input was excited with a random-phase multisine signal, [13], composed of frequencies in the range $f \in [3, 50]$ Hz. The amplitude of this signal was selected to avoid motor current saturation. The scheduling signal is a random multisine as well, with the same period as the system input, that is 8.192 seconds, however with a much more restricted frequency spectrum $f \in [0.1, 1]$ Hz and taking values in the operating range $p \in [-0.1508, 0.0229]$ m, where 0 m corresponds to the middle position of the stage. A global data set then consists of four consecutive signal periods, each comprising 8192 data samples of the reference velocity for the X-motor, measured position of

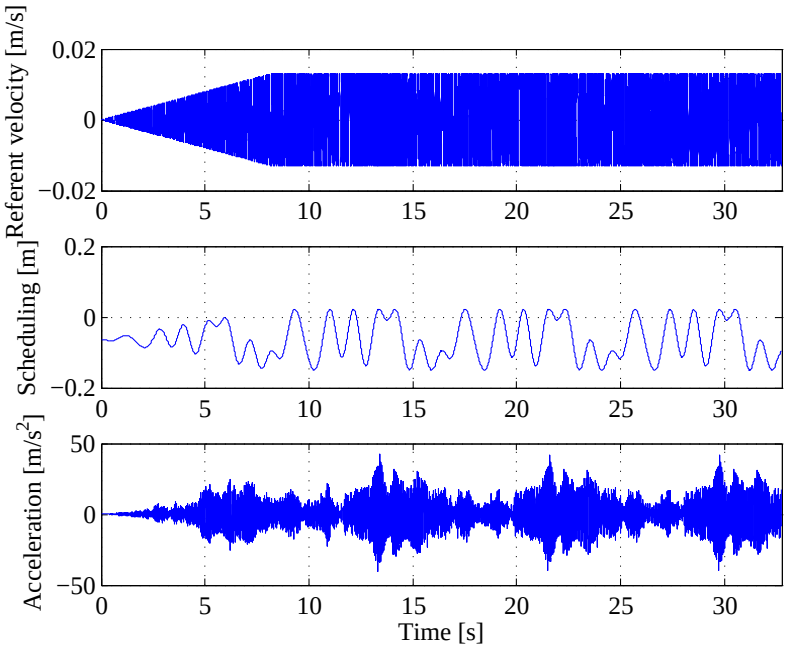

Figure 2: Global data set used for identification.

the Y-motor and the resulting acceleration of the end-effector. The first period differs from the others in the sense that the input is scaled by a ramp signal for a smooth start. Two different realizations of the global experiment were conducted, one for identification (Fig.2) and the other for validation.

The local experiments were performed for fixed values of the scheduling parameter, that is, fixed positions of the Y-motor. Four local experiments, for the positions of the Y-motor equal to

$$p = -0.1508,\ -0.0929,\ -0.0350,\ 0.0229\,\mathrm{m}$$

were performed. The X-motor input signal for each local experiment is a random multisine with the same specifications as for the global experiments. The local identification data are chosen to be used in the frequency domain. The local data set consists of four frequency response functions (FRFs), corresponding to four experiments and evaluated at 385 equally distributed frequency lines of interest ($f \in [3, 50]\,\mathrm{Hz}$).

4.3 Algorithm settings

Solving both (8) and (11) requires an initial estimate of the LPV model parameters (3). This is provided by the SMILE (State-space Model Interpolation of Local Estimates) technique presented in [12], a numerically well-conditioned local identification technique based on the interpolation of a set of local LTI models that are obtained for fixed operating conditions of the system. In our case, these LTI models are obtained using a nonlinear least squares frequency domain linear model identification method [13]. The LTI models are of the fourth order, which dictates the order of the LPV model. Since there was no apriori knowledge about suitable basis functions, and since there are four LTI models to be interpolated, a third-order polynomial scheduling parameter dependency and hence following set of basis functions:

$$f_1 = p(t),\quad f_2 = p(t)^2,\quad f_3 = p(t)^3,$$

was chosen. Through this choice, the interpolation can be performed without introducing errors, that is, the LTI models correspond exactly to the LPV model for the corresponding fixed values of the scheduling

Data set	SMILE	NLS	$\text{NLS}_{\ell_{2,1}}$
Identification	5.6939	1.8009	2.4265
Validation	3.7841	1.7125	2.2579

Table 1: Root mean square error of the models on global identification and validation data.

parameter. Global and local identification data are combined into the objective function (5), with W_{t} and W_{f} normalizing the global and local data, respectively. The global and local data are given the same importance, and $\gamma = 0.1$, (10). Both the NLS combined global and local approach [5] minimizing (5), and its regularized version $\text{NLS}_{\ell_{2,1}}$ solving (12) are applied. Since there is no direct feedthrought between the input and the output due to data sampling, the complete state-space matrix $(\mathscr{D} \diamond p)$ is fixed to zero, in both cases.

4.4 Results

In the first case, the Levenberg-Marquardt algorithm did not converge; it was stopped because the maximum number of iterations (500) had been achieved. The sequential SOCP was stopped after 150 iterations. By looking at Fig. 3 and Table 1, one can see a significant improvement in the global model accuracy achieved with the NLS model (yellow), and with the $\text{NLS}_{\ell_{2,1}}$ (green) model, in comparison with the SMILE model both algorithms start from (red). This is expected given the local nature of the SMILE technique. It also justifies the use of the global data in addition to the local. The NLS model gave smaller global error ($\approx 33\%$), again not surprisingly due to the regularization term the second method accounts for.

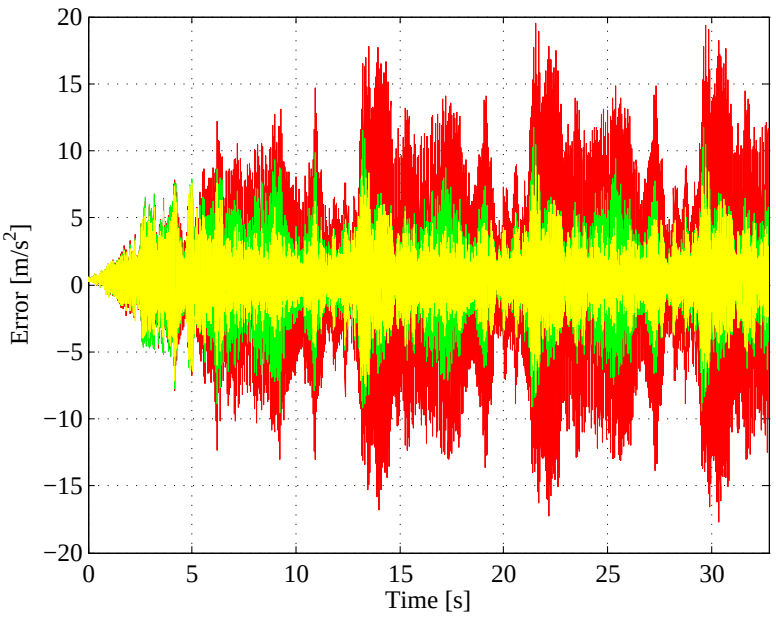

Figure 3: Global identification error of the SMILE model (red), the NLS model (yellow), and the $\text{NLS}_{\ell_{2,1}}$ model (green).

Fig. 4 and Fig. 5 evaluate the models using the local identification data (FRF measurements). The SMILE model performs better than the NLS and $\text{NLS}_{\ell_{2,1}}$ models, expectedly since it comes from a local identification technique. The NLS model is slightly more accurate than the $\text{NLS}_{\ell_{2,1}}$ model.

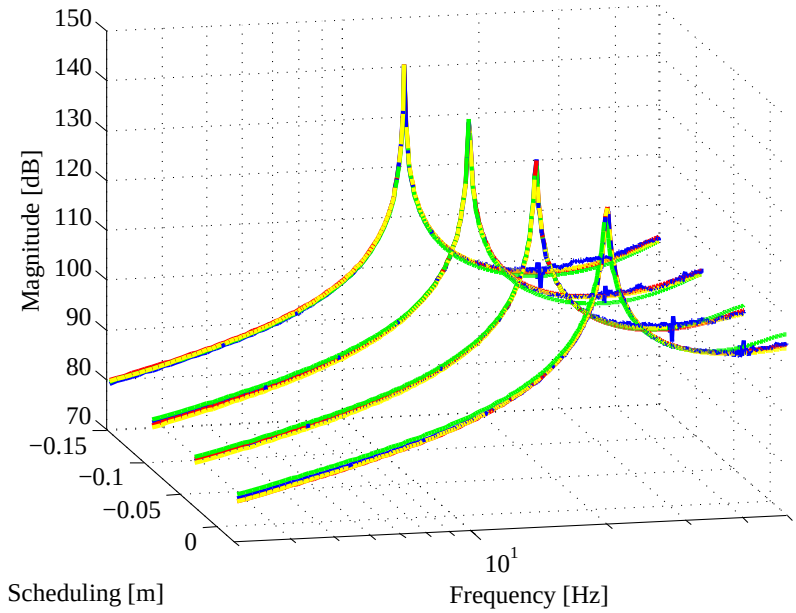

Figure 4: Local identification fit - magnitude. Blue - the measurements, red - the SMILE model, yellow - the NLS model, and green - the $\text{NLS}_{\ell_{2,1}}$ model.

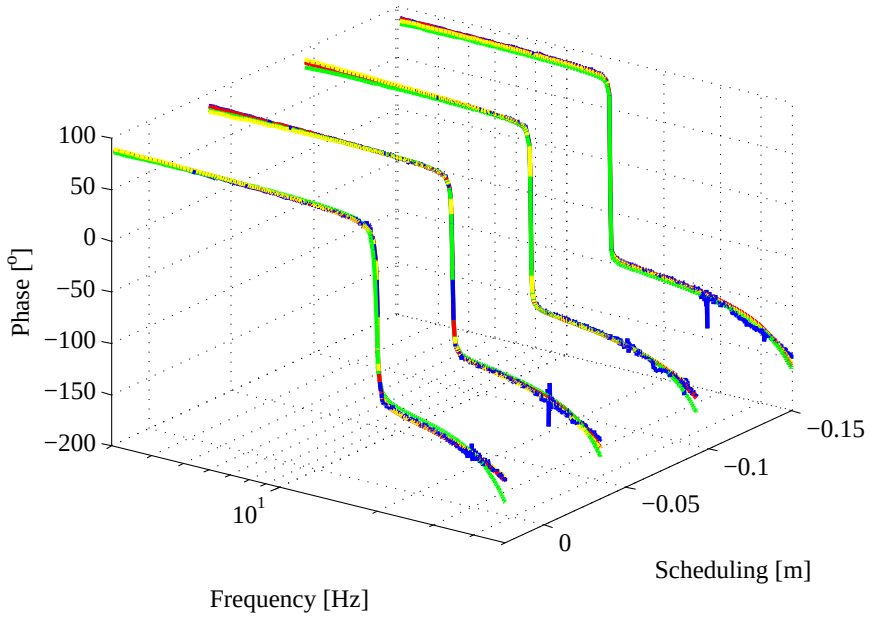

Figure 5: Local identification fit - phase. Blue - the measurements, red - the SMILE model, yellow - the NLS model, and green - the $\text{NLS}_{\ell_{2,1}}$ model.

i	$\|vec(A_i)\|_2$	$\|vec(B_i)\|_2$	$\|vec(C_i)\|_2$	$\|vec(D_i)\|_2$
0	2.6199	1.5710	$1.0573 \cdot 10^5$	0
1	5.0164	1.1724	$8.3054 \cdot 10^5$	0
2	75.6697	31.3980	$1.1995 \cdot 10^7$	0
3	349.4125	337.4616	$6.2491 \cdot 10^7$	0

Table 2: Parameter size of the NLS model.

i	$\|vec(A_i)\|_2$	$\|vec(B_i)\|_2$	$\|vec(C_i)\|_2$	$\|vec(D_i)\|_2$
0	8.8685	45.5739	$3.6141 \cdot 10^5$	0
1	0.0012	$3.1274 \cdot 10^{-9}$	$7.4513 \cdot 10^{-10}$	0
2	0.0046	$2.9059 \cdot 10^{-9}$	$2.4877 \cdot 10^{-9}$	0
3	0.0089	$2.9402 \cdot 10^{-9}$	$3.2437 \cdot 10^{-9}$	0

Table 3: Parameter size of the $\text{NLS}_{\ell_{2,1}}$ model.

Table 2 and 3 give an indication of the size of the parameters of the different parts of the NLS and $\text{NLS}_{\ell_{2,1}}$ models, respectively. Table 2 clearly shows that the values of the parameters in the NLS model are scattered throughout a large range, and throughout the whole model. Table 3 shows that the $\text{NLS}_{\ell_{2,1}}$ model has only system matrix dependend on the scheduling parameter, since the size of parameters in the B_i and C_i (D_i is zero by default because there is no direct feedthrough between the input and the output) ($i = 1,2,3$) is significantly smaller than the size of the parameters in A_0, B_0 and C_0. Hence, it can be stated that the $\ell_{2,1}$ regularization enabled us to select a more appropriate scheduling parameter dependency; the input matrix and the output equation utilize no basis functions and hence can be modeled as being scheduling parameter independent. Keeping in mind the importance of well-conditioning and sparsity in the LPV control design, the proposed regularized NLS-based LPV identification method shows a potential.

Fig. 6 depicts the pole-zero evolution of the NLS model as the scheduling parameter is changing from the minimal to the maximal operating value. What cathes the eye is the unusual and not very realistic trajectory performed by one of the complex-conjugated pairs of poles, which is with the $\text{NLS}_{\ell_{2,1}}$ model completely circumvented (Fig. 7).

5 Conclusion

With the goal of reducing the number of degrees of freedom and consequently avoiding overparameterization during identification of linear parameter-varying systems, the $\ell_{2,1}$-norm regularization of the fully parameterized model matrices is here explored. Reformulation of the optimization problem with added regularization term into a nonlinear second-order cone programming problem, resulted in an approach successfully validated on an XY-motion system. We obtained an LPV model that requires significantly fewer parameters that the nonregularized version, while still being a good approximation of the system behavior for both varying and fixed operating conditions. Future extensions will focus on regaining the accuracy of the nonregularized solution that was here partially traded-off, while keeping the model sparse.

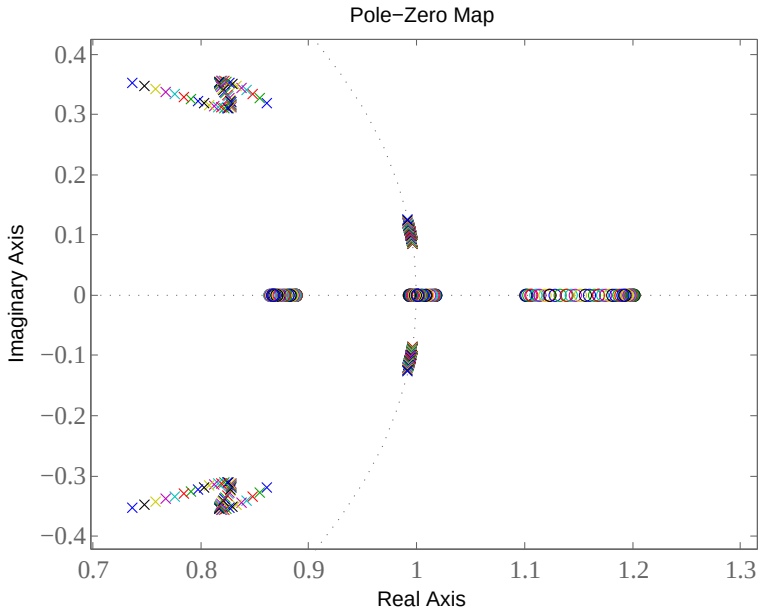

Figure 6: Pole (x) - zero (o) evolution of the NLS model, over the operating range.

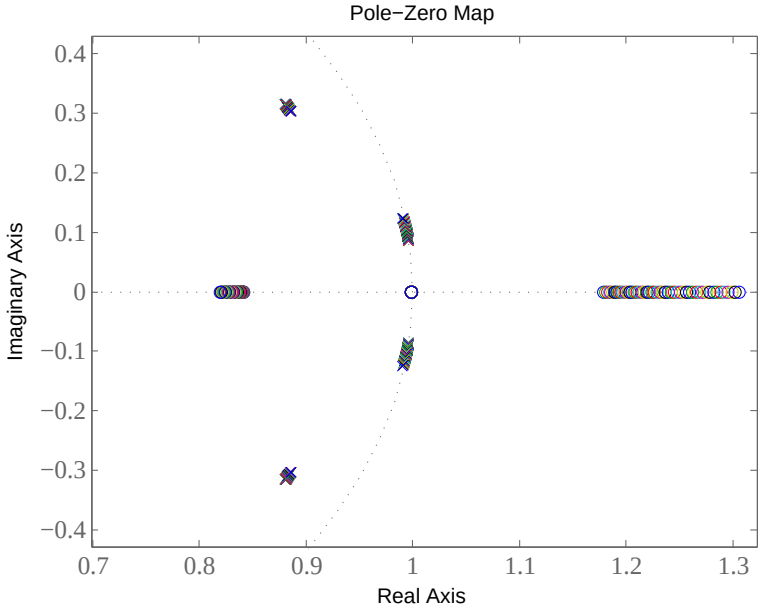

Figure 7: Pole (x) - zero (o) evolution of the model obtained with the $\text{NLS}_{\ell_{2,1}}$ model, over the operating range.

6 Acknowledgement

This research is sponsored by the Fund for Scientific Research (FWO-Vlaanderen) through project G.0002.11, by the KU Leuven-BOF PFV/10/002 Center-of-Excellence Optimization in Engineering (OPTEC), and by the Belgian Program on Interuniversity Poles of Attraction, initiated by the Belgian State, Prime Ministers Office, Science Policy programming (IAP VII, DYSCO).

References

[1] B. Bamieh, L. Giarre, *Identification of linear parameter varying models*, International Journal of Robust and Nonlinear Control, Vol. 12, No. 9, Wiley Online Library (2002), pp. 841-853.

[2] F. Felici, J.-W. Van Wingerden, M. Verhaegen, *Subspace identification of MIMO LPV systems using a periodic scheduling sequence*, Automatica, Vol. 43, No. 10, Elsevier (2007), pp. 1684-1697.

[3] J. De Caigny, R. Pintelon, J. Camino, J. Swevers, *Interpolated modeling of LPV systems based on observability and controllability*, in *Proc. of the 16th IFAC Symposium on System Identification, Brussels, Belgium*, (2013), pp. 1773-1778.

[4] M. Steinbuch, R. Van De Molengraft, A. van der Voort, *Experimental modelling and LPV control of a motion system*, in *Proceedings of the 2003 American Control Conference*, (2003), vol. 2, pp. 1374-1379.

[5] D. Turk, G. Pipeleers, J. Swevers, *A combined global and local identification approach for LPV systems*, IFAC-PapersOnLine, Vol. 48, No. 28, Elsevier (2015), pp. 184-189.

[6] J. Goos, J. Lataire, R. Pintelon, *Estimation of Linear Parameter-Varying affine state space models using synchronized periodic input and scheduling signals*, in *American Control Conference (ACC), 2014*, (2014), pp. 3754-3759.

[7] R. Tóth, H. Hjalmarsson, C. R. Rojas, *Order and structural dependence selection of LPV-ARX models revisited*, in *2012 IEEE 51st Annual Conference on Decision and Control (CDC)*, (2012), pp. 6271-6276.

[8] P. Gebraad, J.-W. van Wingerden, M. Verhaegen, *Sparse Estimation for Predictor-Based Subspace Identification of LPV Systems*, in *16th IFAC Symposium on System Identification*, (2012), pp. 1749-1754.

[9] M. S. Lobo, L. Vandenberghe, S. Boyd, H. Lebret, *Applications of second-order cone programming*, Linear algebra and its applications, Vol. 284, No. 1, Elsevier (1998), pp. 193-228.

[10] H. Kato, M. Fukushima, *An SQP-type algorithm for nonlinear second-order cone programs*, Optimization Letters, Vol. 1, No. 2, Springer (2007), pp. 129-144.

[11] A. Domahidi, E. Chu, S. Boyd, *ECOS: An SOCP solver for embedded systems*, in *European Control Conference (ECC)*, (2013), pp. 3071-3076.

[12] J. De Caigny, J. F. Camino, J. Swevers, *Interpolating model identification for SISO linear parameter-varying systems*, Mechanical Systems and Signal Processing, Vol. 23, No. 8, Elsevier (2009), pp. 2395-2417.

[13] R. Pintelon, J. Schoukens, *System identification: a frequency domain approach*, John Wiley & Sons (2012).